

Microstructures and properties of A356–10%SiC particle composite castings at different solidification pressures

Pu-yun DONG, Hai-dong ZHAO, Fei-fan CHEN, Jun-wen LI

National Engineering Research Center of Near-net-shape Forming for Metallic Materials,
South China University of Technology, Guangzhou 510640, China

Received 9 July 2012; accepted 15 November 2012

Abstract: A356-based metal matrix composites with 10% SiC particles of 10 μm were fabricated by stir casting and direct squeeze casting process under applied pressures of 0.1 (gravity), 25, 50 and 75 MPa. The microstructures and mechanical properties of the as-cast and T6 heat-treated castings were investigated. The results show that as the applied pressures increase, the casting defects as particle-porosity clusters reduce and the incorporation between the particles and matrix can be improved. The tensile strength, hardness, and coefficients of thermal expansion (CTE) increase with the increase of the pressures. Compared with the as-cast composite castings, the tensile strength and hardness of the heat-treated casting are improved whereas CTEs tend to decrease in T6-treated condition. For the gravity cast composites, there are some particle-porosity clusters on the fracture surface, and the clusters are hardly detected on the fracture surface of the samples solidified at the external pressures. Different fracture behaviors are found between the composites solidified at the gravity and imposed pressures.

Key words: metal matrix composites; squeeze casting; microstructures; mechanical properties

1 Introduction

A356–SiC_p metal matrix composites have received much research interest due to their excellent mechanical properties. A356–SiC_p metal matrix composites can be fabricated by power metallurgy, spray forming, pressure infiltration, pressureless infiltration, and casting and so on [1–4]. In these processes, casting is recognized as an effective method to economically produce large quantities and relatively complex shaped A356–SiC_p metal matrix composites [5]. However, some defects such as porosities and particle agglomeration usually occur in the composite castings [6,7]. Squeeze casting process is an improved technique combining casting and forging advantages, in which shrinkage porosity can be reduced [8–10]. It is also regarded as a near net-shape fabrication process and has been steadily spotlighted in industry application with high performance. Although researchers have contributed a lot of works to the preparation and mechanical properties of Al-based composites [11–14], microstructures and mechanical properties of composite castings fabricated by squeeze

casting are limited and desirable.

In this study, A356–10%SiC_p composite castings were produced by squeeze casting process. Microstructures and mechanical properties as well as CTEs of the as-cast and T6-treated castings were evaluated. The fracture behaviors of the composites were analyzed and discussed.

2 Experimental

In the present study, A356 alloys and SiC particles with average size of about 10 μm were chosen as matrix material and reinforced particles, respectively. The actual chemical compositions of the used A356 alloy are listed in Table 1. In order to improve the wettability of SiC particles, the particles were oxidized by heating at 900 °C for 5 h before addition to the slurry. First, A356 alloys were melted in a graphite crucible inside a resistance heating crucible furnace. After melting, the A356 melt was degassed, and then cooled to 600 °C with a semi-solid state. The SiC particles were added to the semi-solid slurry by using a stainless steel three-blade impeller coated with a zinc oxide. Then the composite

melts was reheated to 670 °C and stirred again for 30 min in argon gas protection. After the second stirring, the melt was fluxed and degassed at 650 °C. During the squeeze casting process, the composite melt was poured into die preheated to 200 °C with a cylindrical cavity of 80 mm in diameter. Then a 1000 kN press with a PLC controller was used for applying different pressures on the composite melt. In the experiment, the squeeze pressures of 0.1 (atmospheric pressure), 25, 50 and 75 MPa were applied on the solidifying castings for 30 s. The obtained squeeze castings with 75 mm in height and obtainment of samples for property analysis in each sample are shown in Fig. 1. The castings were vertically divided into two halves and one half was subjected to a standard T6 heat treatment of A356 alloy including: solution treatment at (535±5) °C for 8 h; quenching in water at room temperature; immediate aging at 180 °C for 6 h; air cooling.

Table 1 Chemical composition of matrix alloy (mass fraction, %)

Si	Mg	Zn	Fe	Mn	Ni
6.84	0.22	0.01	0.12	<0.01	<0.01
Sn	Pb	Ti	Cr	Al	
<0.01	0.01	0.12	<0.01	Bal.	

A Leica DM1 5000 M microscope was employed for observing the microstructure and analyzing the particle distribution. The Academes' Law was applied to measuring the casting densities through weighing small sample from each casting in air and water using a Sartorius-BS224S microbalance with an accuracy of 0.0001 g. Hardness measurement was carried out with a HB-3000B Brinell hardness tester. In the measurement, over 10 fields on each sample were measured and then averaged.

The samples for CTE analysis were machined as 25 mm in length and 6 mm in diameter. The CTE test was performed on a DIL 402C dilatometer (NETZSCH Corp.) with a heating rate of 5 °C/min. During the test, a nitrogen atmosphere with a flowing rate of 30 mL/min was used to keep the chamber temperature consistent. Based on the measured curves of relative length changes versus temperatures, the CTE was calculated between room temperature (RT) and 500 °C. To diminish systematic errors, the dilatometer was calibrated by measuring an alumina sample under identical conditions.

Several tens of tensile samples with a cross section of 5 mm × 3 mm and gauge length of 22 mm were machined from the castings. Room temperature tensile test was conducted at a cross-head speed of 2 mm/min using SHIMADZU AG-X 100KN. The fractured surfaces of the tensile samples were observed and analyzed with a FEIQuanta200 environmental scanning electron microscope (SEM).

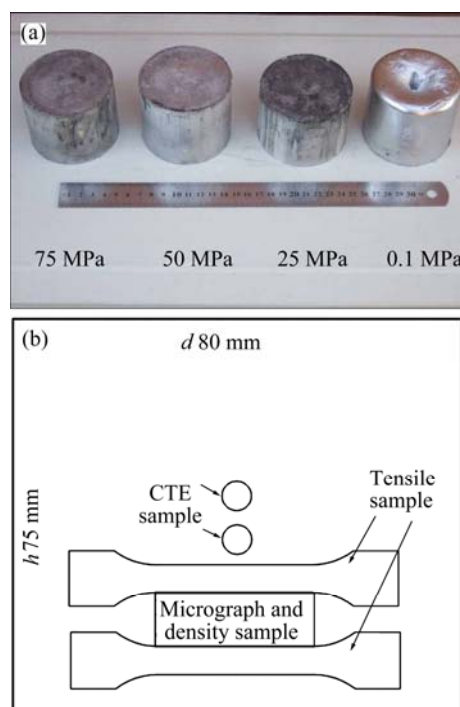


Fig. 1 Experiment composite parts of squeeze casting (a) and sampling positions (b)

3 Results and analysis

3.1 Microstructure

Figure 2 shows the microstructures of the as-cast and T6-treated composite casting at different squeeze pressures. The microstructures are mainly composed of $\alpha(\text{Al})$, eutectics silicon and randomly distributed black SiC particles. Particle-porosity clusters can be clearly observed in the both as-cast and T6-treated samples fabricated at atmospheric pressure shown by the arrows in Fig. 2(a). Particles associated with porosity can be clearly seen at the porosity edge. The reason is that wetting angle between SiC particles and air is 62° [15]. During the composite stirring, a longer stirring time can increase the number of air bubbles entrapped into molten metal and SiC particles are prone to associate with these bubbles. It was reported that an external squeeze pressure during solidification can result in inducing interdendritic flow and hence improve feeding capability minimizing or eliminating shrinkage porosities. As for the composites, the induced squeeze pressure can force the liquid composites melt to flow into the voids of particle-porosity cluster. As a result, particle-porosity clusters disappeared during the solidification with the external pressures in Figs. 2(b), (c) and (d). The $\alpha(\text{Al})$ cells are also refined with the increasing pressures. As can be seen in Fig. 2, compared with the gravity-cast composites, agglomeration distribution of the particles in the squeeze castings is seldom observed. As for the squeeze castings, the imposed pressures caused the interdendritic flow and

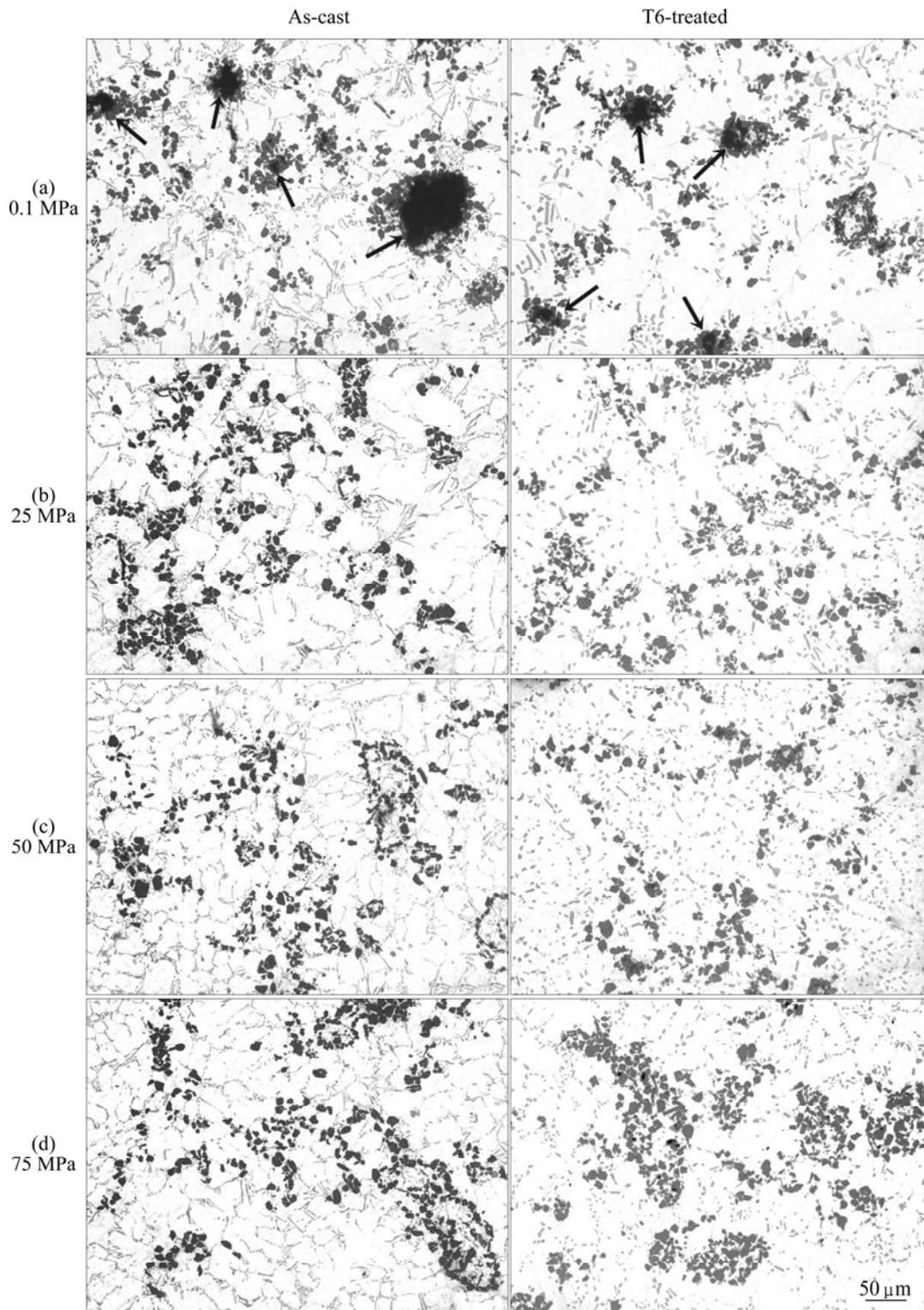


Fig. 2 Metallographs of A356–10%SiC_p composites with different applied solidification pressures

decreased particle-porosity clusters. Meanwhile, the cooling rate of the squeeze casting was higher than that of gravity casting, which is favor of engulfment of SiC particles into dendrites by solid/liquid growth interface [16]. The above two factors contributed to the improved particle distribution in the squeeze castings. After the T6 heat treatment, the eutectics silicon in the composites had

changed from acicular and fibrous to small granular and distributed in the matrix more uniformly. As expected, the heat treatment did not change the SiC particle distribution.

Figure 3 displays the microstructures of the gravity composite castings at high magnification. It can be seen that many eutectic silicon particles associate with SiC

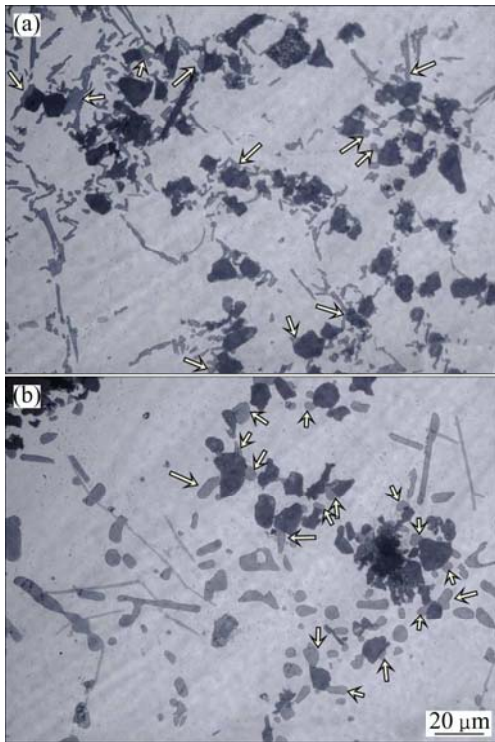


Fig. 3 Microstructures of gravity composite castings: (a) As-cast; (b) T6-treated

particles in the grain boundary indicated by the arrows in the figure. This indicates that the SiC particles act as substrates for heterogeneous nucleation of Si phase, which is coincided with the results in Refs. [16–18]. ZHOU and XU [17] proposed the reason that SiC particles have a lower thermal conductivity compared with aluminum melt and thus the cooling rate of SiC particles is slower than Al liquid alloy so that the particle temperature is higher than the liquid making liquids around the particles solidify in the last stage with eutectic transformation. The nucleation of $\alpha(\text{Al})$ phase starts in the liquid with lower temperature at a distance to the particles. The growth of $\alpha(\text{Al})$ phase makes remaining liquid around SiC particles rich in Si in later solidification stage. Therefore, SiC particles may become the heterogeneous nucleation sites of eutectic silicon phase. In addition, the SiC particles used in the present experiment had been applied to the oxidation treatment forming a continuous homogeneous coating of SiO_2 on the surface. The interfacial reaction between Al liquid and SiO_2 could generate Al_2O_3 and Si [19]. In our viewpoints, this reaction also promotes the nucleation of Si particles on the particles.

3.2 Density and porosity

According to the theoretical density of A356–10%SiC_p of 2.73 g/cm^3 , the porosity content for each casting was calculated with the measured casting densities. Table 2 shows the casting densities and

porosity at the different pressures. The gravity cast composites have the lowest density and highest porosity. This also can be confirmed with the microstructure in Fig. 2(a). Since voids of particle–porosity clusters can be filled with liquid composite melt by induced high pressure, the porosities are decreased with the increasing pressures as shown in Table 2.

Table 2 Densities and porosities of composite castings

Squeeze pressure/MPa	Measured density/($\text{g}\cdot\text{cm}^{-3}$)	Porosity/%
0.1	2.615	4.20
25	2.619	4.10
50	2.639	3.40
75	2.644	3.20

3.3 Coefficients of thermal expansion (CTE)

Figure 4 shows the CTEs measured between RT and $250 \text{ }^\circ\text{C}$ of the both as-cast and T6-treated composites, indicating that the CTE increases with increasing the squeeze pressures. In the case of SiC particle reinforced aluminum matrix composites, the composite thermal expansion behavior is influenced by both the matrix and tightened restriction of the particles. It is known that applied squeeze pressures improve casting–die contact and reduce their air gap. WU [20] researched the interfacial heat transfer coefficients of A356 under different squeeze pressures, and found that the coefficients increased as the pressure increased. The applied pressure and fast solidification rate would bring about larger thermal residual stress for squeeze castings. During the CTE experiment, the residual stress release causes larger strain and CTE value for squeeze castings [21]. So, the composite CTE increases as the applied pressure increases. Compared with the as-cast composites, the T6 heat-treated composites have lower CTE values as shown in Fig. 4 due to release of the residual stress within the heat treatment.

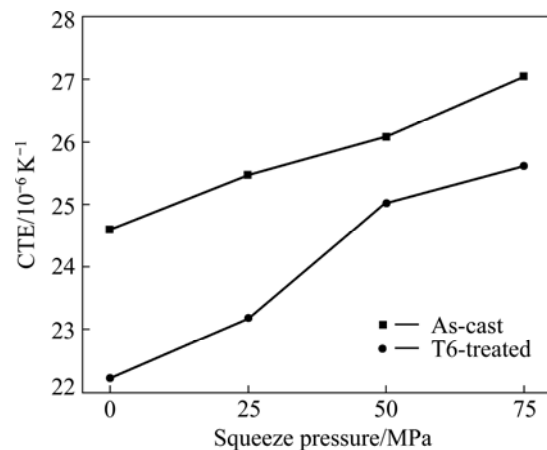


Fig. 4 Effect of applied pressures on CTEs of castings

Microvoids also affect the overall CTE of composites [22,23]. HATTA et al [23] provided a mechanism of reduction in CTE of composite due to voids. Because of different CTEs between SiC particles and A356 matrix, when composites are subjected to temperature rise, the SiC particles and A356 matrix will undertake compressive and tensile stress, respectively. If there are voids in the composites, they also suffer compressive stress from the expansion of composite matrix. The voids can reduce the matrix expansion stress by declining their volumes. Consequently, composite CTE is reduced. Furthermore, the more the porosity content in composites, the lower the net volume of composites, resulting in lower expansion during CTE tests. Figure 5 plots the CTE and porosity of the composites. It is indicated that the composite CTE increases as the porosity decreases.

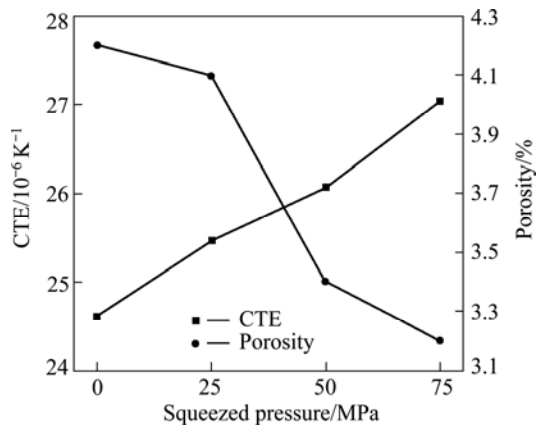


Fig. 5 Relationship of CTE and porosity in as-cast composites

3.4 Mechanical properties

As shown in Table 3, the tensile strengths and elongations of the both as-cast and T6-treated A356–10%SiC_p increase with increasing the squeeze pressure. As well known, high squeeze pressure applied to solidifying castings can eliminate porosity, and increase cooling rate by improving melt and die contact and achieve fine and uniform grain size contributing to improve mechanical properties. In particle reinforced composites, dislocation due to mismatch in thermal

Table 3 Tensile strength, elongation and hardness of composites

Pressure/ MPa	Tensile strength/MPa		Elongation/%		Hardness, HBS	
	As-cast	T6- treated	As-cast	T6- treated	As-cast	T6- treated
0.1	129.327	174.300	1.726	2.057	55.89	65.21
25	165.530	206.600	1.737	3.954	62.10	74.09
50	165.895	205.991	2.212	5.492	64.49	77.69
75	195.096	224.585	3.500	7.615	66.28	77.23

expansion between SiC particles and matrix materials is also an important factor affecting mechanical properties. The increasing cooling rate caused by the squeeze pressure led to large undercooling [24,25]. As a result the composites contain more dislocations in SiC particles and matrix interface under the applied pressures.

Table 3 also indicates that the tensile strength increased remarkably after T6 treatment. During solution stage of T6 treatment, supersaturated and homogenized solid solution is obtained and more Mg₂Si phase was dissolved into the Al-matrix. According to Fig. 2, the Si particles in the as-cast castings were of coarse and acicular needle-like morphologies. During the solution heat treatment, the particles changed from acicular to small granular through fragmentation, spheroidization and coarsening. The above two factors are contributed to the improved properties of the heat-treated composites.

The results of measured hardness are listed in Table 3. The squeeze cast composites have higher hardness than the gravity ones. Under the squeeze pressures, the voids of particles-porosity clusters were filled and more particles undertook the hardness test loading. After T6 heat treatment, the composite hardness increased. This is due to dissolving of silicon particles into α (Al) during the aging period.

3.5 Fractography

Figure 6 shows the fracture morphologies of the

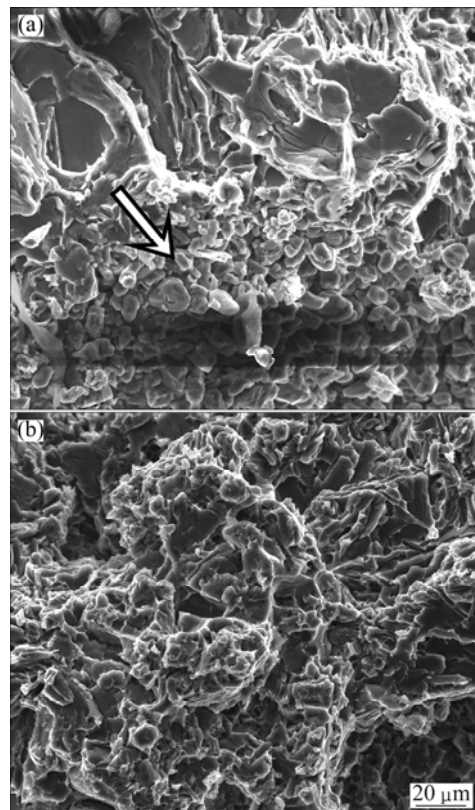


Fig. 6 Fracture morphologies of as-cast A356–10%SiC_p composites: (a) 0.1 MPa; (b) 75 MPa

as-cast composites. Under the gravity condition, the composite fracture surface is composed of particle–porosity cluster (shown by arrow), cleavage facets and lots of secondary cracks are shown in Fig. 6(a), clearly indicating a brittle fracture mode. Because the particle–porosity cluster can reduce casting effective load area and induce local stress concentration in surrounding matrix, they should act as sites for crack initiation. On the fracture surface of the squeeze cast composites (Fig. 6(b)), particle–porosity cluster were not observed but small cleavage facets and secondary cracks can still be found.

Figure 7 shows fractographs of the composites after the T6 treatment. With regard to the gravity cast composites, particle–porosity clusters are also to be found acting as crack initiation sites. The appearance of slip band in Fig. 7(a) indicated plastic flow in the tensile test. As for the composite solidified under 75 MPa, lots of shallow dimples and slip bands can be observed (see Fig. 7(b)), showing a ductile mode fracture.

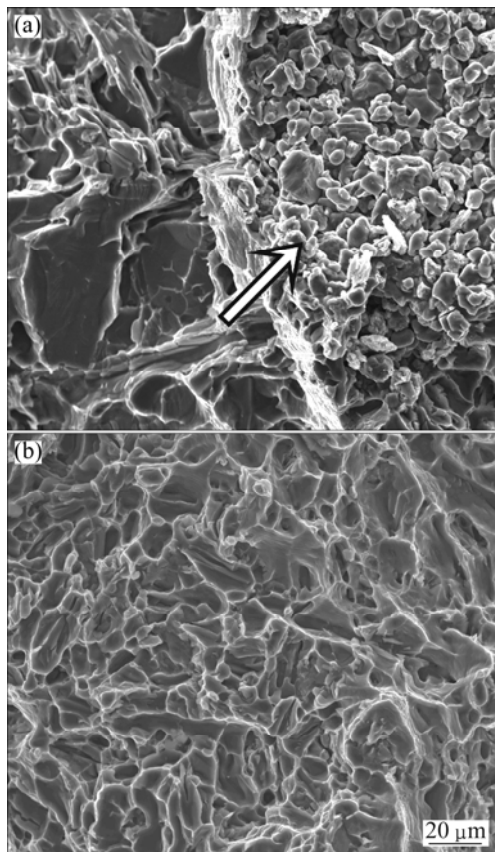


Fig. 7 Fracture morphologies of T6-treated A356–10%SiC_p composites: (a) 0.1 MPa; (b) 75 MPa

4 Conclusions

1) The A356-based composites with 10% SiC particles of 10 μm were fabricated by stir casting and direct squeeze casting process. The squeeze pressures

can reduce the particle–porosity clusters and refine the grains. Hence, the composite tensile properties, hardness, elongation and CTEs increased with the increase of the squeeze pressures.

2) Compared with the as-cast composite castings, the tensile strength and hardness of the heat-treated casting were improved whereas CTEs tended to decrease in T6-treated condition.

3) It is clearly observed that for the gravity cast composites there are some particle–porosity clusters on the fracture surface and the clusters were hardly detected on the fracture surface of the samples solidified at the external pressures.

4) Different fracture behaviors were found between the composites solidified at the gravity and imposed pressures. As for the gravity cast composites, fracture cracks were always originated from particle–porosity clusters as a brittle mode. The squeeze cast composites show brittle mode fracture in as-cast condition while shallow dimples and slip bands can be observed in the composites after T6 treatment, indicating a ductile mode.

References

- [1] LLOYD D J. Particle reinforced aluminum and magnesium matrix composites [J]. *Int Mater Rev*, 1994, 39: 1–23.
- [2] CHEN Cong-cong, CHEN Gang, YAN Hong-ge, SU Bin. Friction and wear properties of particle reinforced graded aluminum matrix composite [J]. *The Chinese Journal of Nonferrous Metal*, 2011, 21(6): 1258–1264. (in Chinese)
- [3] ZHANG Z, CHEN X G, CHARETTE A. Particle distribution and interfacial reactions of Al–7%Si–10%B₄C die casting composite [J]. *J Mater Sci*, 2007, 42: 7354–7362.
- [4] WANG Qing-ping, WU Yu-cheng, HONG Yu, PAN Rong-jun, MIN Fan-fei. Microstructures and bending properties of Al composites with high volume fraction of SiC_p [J]. *The Chinese Journal of Nonferrous Metal*, 2010, 20(2): 239–243. (in Chinese)
- [5] HASHIM J, LOONEY L, HASHMI M S J. Particle distribution in cast metal matrix composites—Part I [J]. *J Mater Process Tech*, 2002, 123(2): 251–257.
- [6] HASHIM J, LOONEY L, HASHMI M S J. Metal matrix composites: Production by the stir casting method [J]. *J Mater Process Tech*, 1999, 92–93: 1–7.
- [7] SURAPPA M K. Microstructure evolution during solidification of DRMMCs (discontinuously reinforced metal matrix composites): State of art [J]. *J Mater Process Tech*, 1997, 63(1): 325–333.
- [8] RAJAGOPAL S. Squeeze casting: A review and update [J]. *J Appl Metalw*, 1981, 1(4): 3–14.
- [9] GHOMASHCHI M R, VIKHROV A. Squeeze casting: An overview [J]. *J Mater Process Tech*, 2000, 101(1): 1–9.
- [10] SEVIK H, CAN KURNAZ S. Properties of alumina particulate reinforced aluminum alloy produced by pressure die casting [J]. *Mater Des*, 2006, 27(8): 676–683.
- [11] GENG L, ZHANG H W, LI H Z, GUAN L N, HUANG L J. Effects of Mg content on microstructure and mechanical properties of SiC_p/Al–Mg composites fabricated by semi-solid stirring technique [J]. *Transactions of Nonferrous Metals Society of China*, 2010, 20(10): 1851–1855.

- [12] CHOU S N, HUANG J L, LII D F, LU H H. The mechanical properties and microstructure of Al_2O_3 /aluminum alloy composites fabricated by squeeze casting [J]. *J Alloy Compd*, 2007, 436(1): 124–130.
- [13] SU Hai, GAO Wei-li, MAO Cheng, ZHANG Hui, LIU Hong-bo, LU Jian, LU Zheng. Microstructures and mechanical properties of $SiC_p/2024$ aluminum matrix composite synthesized by stir casting [J]. *The Chinese Journal of Nonferrous Metal*, 2010, 20(2): 217–225. (in Chinese)
- [14] ZHU X M, YU J K, WANG X Y. Microstructure and properties of Al/Si/SiC composites for electronic packaging [J]. *Transactions of Nonferrous Metals Society of China*, 2012, 22(7): 1686–1692.
- [15] ROHATGI P K, RAY S, ASTHANA R, NARENDRANATH C S. Interface in cast metal-matrix composites [J]. *Mater Sci Eng A*, 1993, 162(1–2): 163–174.
- [16] WU Jie-jun, WANG Dian-bin, CUI Jian, YUAN Guang-jiang. Analysis of casting defects in SiCp reinforced aluminum matrix composites [J]. *Acta Metall Sin*, 1999, 35(1): 103–108. (in Chinese)
- [17] ZHOU W, XU Z M. Casting of SiC reinforced metal matrix composites [J]. *J Mater Process Tech*, 1997, 63(1): 358–363.
- [18] STEFANOS M S, AZARIAS A M. Solidification microstructure and heterogeneous nucleation phenomena in cast SiC_p-reinforced hypereutectic Al–Si alloy composites [J]. *Scand J Metall*, 2005, 34(1): 16–21.
- [19] UREÑA A, MARTÍNEZ E E, RODRIGO P, GIL L. Oxidation treatments for SiC particles used as reinforcement in aluminium matrix composites [J]. *Compos Sci Tech*, 2004, 64(12): 1843–1854.
- [20] WU Chao-zhong. Investigation of the interface heat transfer coefficients of aluminum squeeze castings [D]. Guangzhou: South China University of Technology, 2011. (in Chinese)
- [21] SHU K M, TU G C. The microstructure and the thermal expansion characteristics of Cu/SiC_p composites [J]. *Mater Sci Eng A*, 2003, 349(1): 236–247.
- [22] SHEN Y L. Combined effects of microvoids and phase contiguity on the thermal expansion of metal-ceramic composites [J]. *Mater Sci Eng A*, 1997, 237: 102–108.
- [23] HATTA H, TAKEI T, TAYA M. Effects of dispersed microvoids on thermal expansion behavior of composite materials [J]. *Mater Sci Eng A*, 2000, 285(1): 99–110.
- [24] FRANKLIN J R, DAS A A. Squeeze casting—a review of status [J]. *British Foundryman*, 1984, 77(3): 150–158.
- [25] MORTON J R, BARLOW J. Squeeze casting: from a theory to profit and a future [J]. *Institute of British Foundryman*, 1994, 87(1): 23–28.

不同凝固压力条件下 A356–10%SiC 复合材料的 微观组织及性能

董普云, 赵海东, 陈飞帆, 李俊文

华南理工大学 国家金属材料近净成形工程技术研究中心, 广州 510640

摘要: 通过搅拌法制备 A356–10%SiC 复合材料, 并分别在 0.1(重力条件)、25、50 和 75 MPa 压力条件下进行该复合材料的直接挤压铸造成形, 研究了铸态和 T6 热处理后复合材料的微观组织及力学性能。结果表明: 随着挤压力的增大, 铸件的增强颗粒–孔洞团簇缺陷减少, 并改善了增强颗粒与基体间的结合强度, 拉伸强度、硬度和热膨胀系数增加。与铸态复合材料相比, T6 热处理后复合材料的抗拉强度和硬度增大而热膨胀系数减小; 在重力条件下凝固的复合材料断口处存在增强颗粒–孔洞团簇缺陷, 而在挤压力下凝固的复合材料断口未观察到该缺陷, 断口特征表明两者存在不同的断裂机制。

关键词: 金属基复合材料; 挤压铸造; 微观组织; 力学性能

(Edited by Hua YANG)